Acoustic emission source localization in anisotropic structures with diffuse field conditions using a time reversal approach

Francesco Ciampa, Michele Meo[a]

Department of Mechanical Engineering, University of Bath, Bath, UK

[a]m.meo@bath.ac.uk

Keywords: stiffened panel, impact localization, wave propagation, time reversal.

Abstract

This research work presents an *in-situ* imaging method for the localization of the impact point in complex anisotropic structures with diffuse field conditions, using only one passive transducer. The proposed technique is based on the time reversal approach applied to a number of waveforms stored into a database containing the experimental Green's function of the medium. The present method exploits the benefits of multiple scattering, mode conversion and boundaries reflections to achieve the focusing of the source with high resolution. The optimal re-focusing of the back propagated wave field at the impact point is accomplished through a "virtual" imaging process, which does not require any iterative algorithms and a priori knowledge of the mechanical properties of the structure. The robustness of the time reversal method is experimentally demonstrated on a stiffened composite panel and the source position can be retrieved with a high level of accuracy (maximum error less than 3%) in any position of the structure. Its very simple configuration and minimal processing requirements and computational time (less than 1 sec) make this method a valid alternative to the conventional imaging structural health monitoring systems for the acoustic emission source localization.

1. Introduction

Traditionally, the determination of the impact location is an inverse problem achieved by optimization methods based on wave propagation approaches. These techniques are usually divide in two steps. First, the time of arrival (TOA) of the *ballistic waves* (direct waves from the source to the receiver) are recorded by a network of passive transducers. The waveforms are usually analyzed with advanced signal processing techniques and then resolution algorithms can be employed to obtain the impact coordinates. Even though most of these methods are able to find the impact source with satisfactory accuracy in isotropic [1, 2] and anisotropic [3, 4, 5] structures, a number of issues still need to be addressed. At first, they require a relatively large number of transducers, especially in composite materials, wherein the group velocity due to structural anisotropy is angular dependent. Then, only the coherent part of the wave field that arrives first to the sensors is used, regardless the contribution from the remaining part of the signal. Indeed, the dispersive nature of guided Lamb waves, as well as the presence in geometrically complex structures of multiple scattering, reflections from the boundaries and mode conversion (known from seismology as *coda*) can alter the resulting signal, leading to a wrong estimation of the TOA. That is, the wave field of complex structures (with stiffeners, rivets, holes and voids), excited over a finite bandwidth, becomes diffuse incoherent [6]. However, the acoustic emission (AE) propagation can be described in terms of signal processing as a linear system with different impulse responses. Lobkins and Weaver [7] showed that the structural impulse response (Green's function) could be retrieved from the cross-correlation of the elastic diffuse wave field at the sensors location. This concept was widely used in seismology and ultrasonic applications, and only recently it was examined through a time reversal (TR) process.

Based on the principle of time-reversal invariance and spatial reciprocity of the acoustic wave equation in a lossless medium, in a TR experiment, the elastic waves diverging from a point-like target can be focused back to the original source if the output measured by a set of transducers is time reversed and re-emitted back onto the excitation point [8]. Nevertheless, a perfect localization would require a totally covering array of sensors (closed cavity), which is impossible to obtain in practise. Hence, the closed cavity is replaced by a time reversal mirror (TRM) of finite bandwidth and aperture that limits the focusing quality. However, it was illustrated by Derode et al. [9] that the reverberations of a diffuse wave field in a complex medium enhance the focusing resolution of the re-emitted signal. Such a combination of TR and diffusive wave fields is known as Correlation of a Diffuse Field (CDF). From a physical point of view, this phenomenon [10] is due to the presence of scatterers within the medium that allows the *evanescent modes* (waves that decay exponentially with the distance to the source) to be converted in propagating modes. These waves, carrying the information of the impact source to the far field, where the TRM is located, can participate to the focusing process. The result of such operation creates a "virtual" enlargement of the transducers angular aperture (*kaleidoscopic effect*) of the TRM and thus the number of sensors can be drastically reduced.

This paper reports a one-channel imaging method aimed to detect in real time the impact source in complex anisotropic structures with diffuse field conditions. The proposed technique, based on the time reversal approach, allows achieving the optimal focalization of the AE source (impact event) as it overcomes the drawbacks of most impact identification methods. In a first step, the impulsive responses of the medium were acquired and stored into a computer. Then, exploiting the benefits of multimodal conversion and scattering effects, a virtual focusing procedure was performed by using only one passive sensor placed on a generic point of the structure. The robustness of this approach is experimentally demonstrated on a dissipative stiffened carbon-fibre composite panel.

The layout of the paper is as follow: in the next Section, the imaging method for the localization of the impact source is presented. Section 3 reports the experimental set-up whilst Section IV shows the imaging results for two different impact points. Then, the conclusions of the paper are discussed.

2. One channel impact localization algorithm

The idea of using TR as an imaging method of the impact source was originally developed by Ing et al. [11] for the detection of a finger knock on a glass plate. Here, we combine the CDF method with the advantages of a TR process, already used in conventional pulse-echo [12] and imaging [13, 14] damage detection. The presented work represents a SHM technique based on the correlation of the signals representing the experimental Green's function of a reverberant field, measured by only one passive transducer, and its reversed in the time domain. Hence, in order to obtain the optimal re-focusing at the impact source in complex anisotropic structures, the transfer matrix of the structure H(ω) is first introduced, and then TR imaging techniques is analyzed.

2.1. The structural transfer matrix H

The TR process was split into two steps. In a first step, the surface structure ("focusing plane") was entirely divided in M = 50 x 15 "observation points" distributed along a grid at interval of 2 cm. At each point, the acoustic emission was generated by impact loads. (Fig. 1).

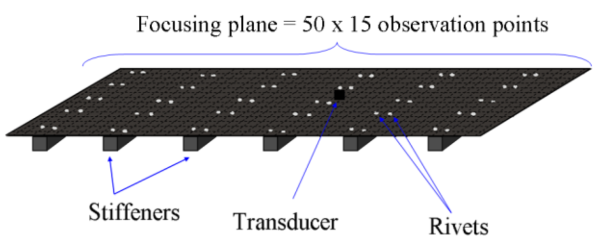

Figure 1 Experimental set-up.

Due to linearity, the acoustic field measured by the transducer from the m^{th} observation point is:

$$f(t)=\sum_{m=1}^{M}\mathbf{h}_m(t)\otimes\mathbf{e}_m(t)=\int_{-\infty}^{-\infty}\sum_{m=1}^{M}\mathbf{h}_m(\tau)\mathbf{e}_m(t-\tau)d\tau \quad (1)$$

where the symbol "⊗" represents a temporal convolution and $\mathbf{h}_m(t)$ ($1\leq m\leq M$) is the linear propagator operator defining the Green's function measured by the sensor. This term includes all the propagation effects through the medium from the m^{th} observation point to the receiver (included its acoustic-electric response). $\mathbf{e}_m(t)$ is the column vector of the input signal sent by the m^{th} source on the focusing plane and $f(\omega)$ is the output signal measured by the transducer at each instant in time. In the frequency domain, equation (1) is:

$$F(\omega)=\sum_{m=1}^{M}\mathbf{H}_m(\omega)\mathbf{E}_m(\omega) \quad (2)$$

which can be written in matrix form as:

$$\underbrace{F(\omega)}_{1\times 1}=\underbrace{\mathbf{H}_m(\omega)}_{1\times M}\underbrace{\mathbf{E}_m(\omega)}_{M\times 1} \quad (3)$$

where the matrix $\mathbf{H}_m(\omega)$ is the *transfer matrix* of the system (Fourier transform of the Green's function) and represents the amplitude of the i-th guided Lamb mode associated to the i-th eigenfrequency. For the spatial reciprocity condition, the transpose of $\mathbf{H}_m$ ($\mathbf{H}_m^T$) corresponds to the propagation between the transducer and the observation points (Fig. 2):

$$\mathbf{E}_m(\omega)=\mathbf{H}_m^T(\omega)F(\omega) \quad (4)$$

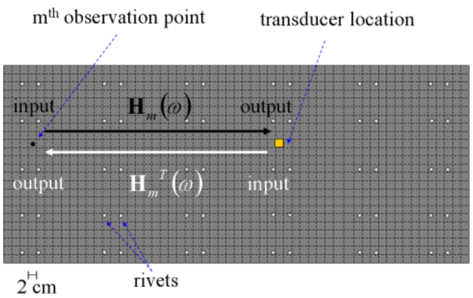

Figure 2 Reciprocity condition of the transfer matrix H(ω).

Hence, the M signals representing a library of impulse responses $\mathbf{H}_m(\omega)$ of the structure were recorded by the transducer and stored into the computer memory.

2.2. Time reversal focusing approach

The second step consisted in recognition of the optimal refocusing procedure at the source location. The basic idea was to time reverse not only the Green's function associated to the AE source, but also to neighbouring points (observation points). Thereby, a new impact was applied in one of the points (of unknown location) of the focusing plane and its impulse response was measured by the sensor. TR behaves as a spatio-temporal matched filter that maximizes the ratio between the amplitude of the output signal (waveform acquired) and the square root of the input energy (impulse applied). Hence, assuming that the impact source in the second step is located at m_0, the input column vector $\mathbf{e}_{m0}(t)$ from the m^{th} observation point can be mathematically approximated to a temporal delta function $\delta(t)$ only when $m = m_0$. In the frequency domain, the emitted signal is $\mathbf{E}_{m0}(\omega)=\{0,\ldots 0,1,0,\ldots 0\}$. According to (3), the wave field received by the transducer is:

$$F_{m0}(\omega)=\mathbf{H}_{m0}(\omega)\mathbf{E}_{m0}(\omega) \quad (5)$$

and the Time Reversal (TR) operation of the Green's function [$\mathbf{h}_{m0}(-t)$] in the time domain is equivalent to taking its complex conjugate in the Fourier domain. Hence, time reversing the spectrum of the transducer output, we have:

$$F_{m0}^*(\omega)=\mathbf{H}_{m0}^*(\omega)\mathbf{E}_{m0}^*(\omega)=\mathbf{H}_{m0}^*(\omega)\mathbf{E}_{m0}(\omega) \quad (6)$$

where the superscript '*'denotes complex conjugate and $\mathbf{E}_{m0}(\omega)$ is real. Combining equations (4) and (6), the back-propagated signal at the source is:

$$\mathbf{E}_{TR}(\omega) = \mathbf{H}_m^{\ T}(\omega) F_{m0}^{\ *}(\omega) = \mathbf{H}_m^{\ T}(\omega) \mathbf{H}_{m0}^{*}(\omega) \mathbf{E}_{m0}(\omega) \qquad (7)$$

and $\mathbf{H}_m^{\ T}(\omega)\mathbf{H}_{m0}^{*}(\omega)$ is called the TR operator. Since equation (7) has a maximum at the focus point, the information associated to the AE source location can be extracted from a "virtual" TR experiment. Fig. 3 illustrates the procedure for obtaining the imaging focusing with a TR analysis.

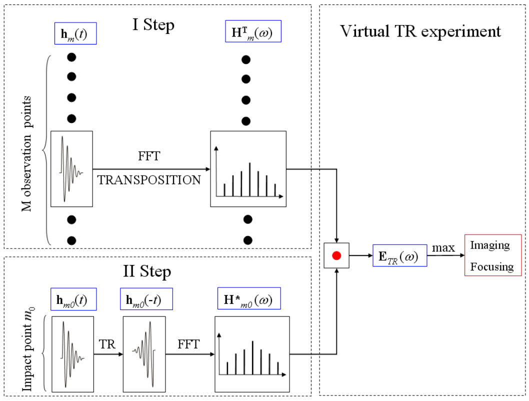

Figure 3 Architecture of the time reversal imaging process.

3. Experimental set-up

The experiments were carried out on a reverberant carbon-fibre composite plate (100cm x 30 cm x 3 mm) reinforced with six vertical stiffeners and connected with rivets (7.9 mm of diameter) (Fig. 4). For the library of signal needed to implement the technique, the impacts were applied to 750 observation points spaced 2 cm apart using a hand-held modal hammer, manufactured by Meggit-Endveco. The experimental Green's function from each observation point was acquired using an acoustic emission sensor instrumented with an oscilloscope (Picoscope 4224) with a sampling rate of 25 MHz. The passive sensor employed was a surface bonded acoustic emission sensor with a central frequency of 300 kHz. The transducer output was connected to a pass-band filter with a frequency bandwidth between 200 and 400 kHz and a preamplifier. According to the d_{31}/d_{32} electromechanical coupling mechanism of the acoustic emission sensor, at the mentioned finite bandwidth, only the fundamental antisymmetric Lamb wave A_0 was measured. The time histories of the signal received by the sensor were stored on a computer and processed using a Matlab software code implemented by the authors. All the impacts were carried out manually (with different forces applied) in order to avoid damaging the structure. In addition, as it can be seen from Fig. 5, the signals were normalized in amplitude and averaged in the first step. Due to the long reverberation present in the waveform, the time window of the signals was chosen at 100 ms.

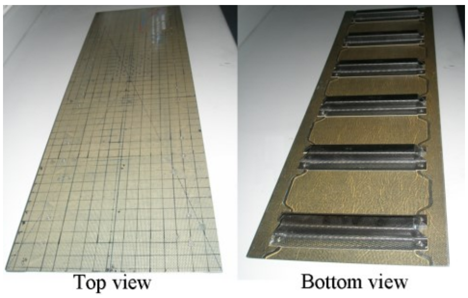

Figure 4 Top and bottom view of the stiffened carbon-fibre composite panel used in the experiments.

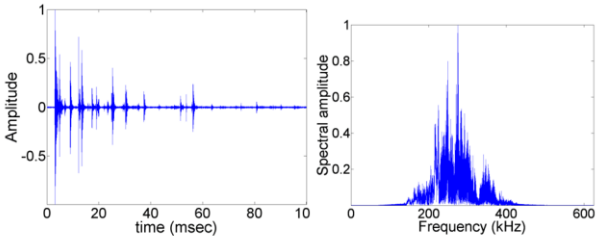

(a) (b)

Figure 5 (a) (b) Normalized time history (a) of one the focusing point and its frequency content (b). In figure (a), a reverberant impulse response is clearly visible.

Table 1

	X-coordinates [cm]	Y-coordinates[cm]
Sensor position (case I1)	60	16
Sensor position(case I2)	24	14
Impact I1	40	10
Impact I2	80	26

4. Imaging localization results

The imaging results are illustrated in Fig. 6. According to Section 2, the refocusing diffused wave field at the source location is represented by a 2-D map and the maximum of $\mathbf{E}_{TR}(\omega)$ [Eq. (7)] is deduced from the values nearest to 1 (characterized by a dark red colour) with a computational time lower than 1 sec.

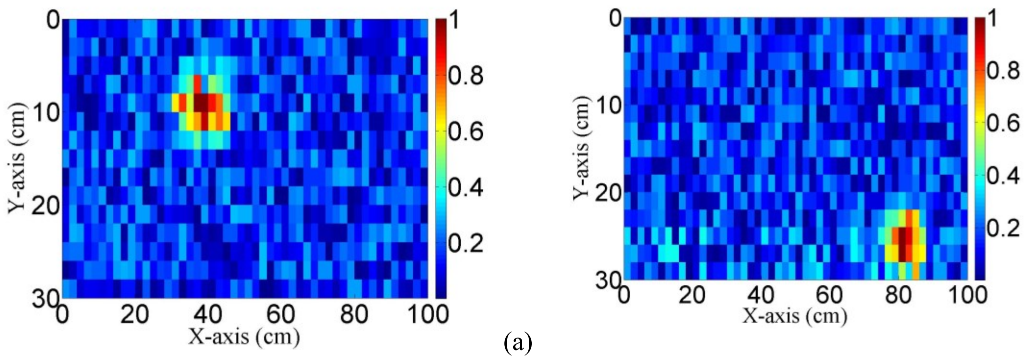

Figure 6 (a) (b) 2D map of the optimal refocusing with a simulated TRA experiment for impact I1 (a) and I2 (b).

From the above figure, it can be clearly seen that the TRA method provides an optimal focusing with reasonable accuracy and the maximum error in estimation of the source location was less than 3% (maximum percentage error given by the error function expressed in [5]) for all the case tested. In fact, as it can be observed from Fig. 6, a maximum value of the refocusing equal to 1 was found even in points close to the true impact source (see the points at x = 38 cm and y = 10 cm for case I1 and x = 80 cm and y = 28 cm for case I2). Such ambiguity might be due to the non-linear attenuation with the wave amplitude that induces distortions of the wave front propagating in the structure [15]. However, a combination of the physical principles of a correlation diffuse field (CFD) technique with the advantages of a time reversal process has shown to provide an optimal re-focusing at the impact location. In other words, the "benefits" of multiple scattering from rivets and modal conversion due to the presence of stiffeners (ultrasonic diffused wave field) allow achieving a high refocusing quality of the recompressed waves without the need to increase the number of sensors for improving the spatial resolution [16]. In fact, from Fig. 7, the correlation coefficients pattern along the X and Y-axis shows that a high resolution can be achieved even using only one passive transducer. Therefore, a very simple configuration is needed for the identification of the AE source, leading to an effective decrease of the number of sensors employed, resulting into costs savings and weight reduction.

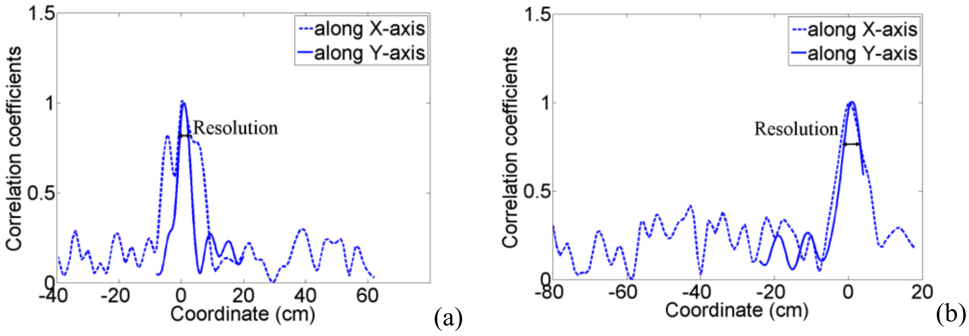

Figure 7 (a) (b) Correlation coefficients pattern along the X and Y-axis with the maximum at the focus point for impact I1 (a) and impact I2 (b).

Nevertheless, during the experiments it was observed that a decrease of the number of observation points led to an increase of the maximum error in retrieving the impact location, with lower values of *max* $\mathbf{E}_{TR}(\omega)$ compared to the previous case (Fig. 8).

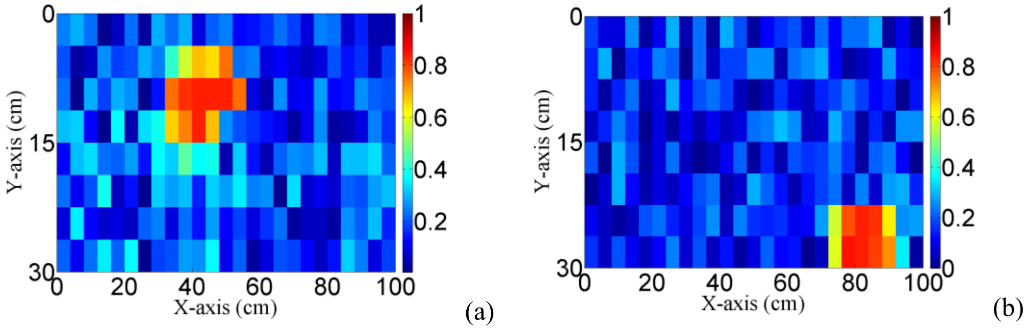

Figure 8 (a) (b) 2D map of the optimal refocusing with a simulated TRA experiment for impact I1 (a) and I2 (b) with 200 observation points.

In particular, assuming 200 observation points the location error was found nearly 10% for impact I1 (Fig. 8-a) and approximately 12% for impact I2 (Fig. 8-b). Hence, unlike other impact localization systems, this method presents the great advantage that it does not require any iterative algorithms as well as a priori knowledge of the mechanical properties, lay-up and anisotropic angular-group velocity pattern of the medium.

Conclusions

In this paper, an *in situ* imaging method able to detect in real-time the impact source in dissipative complex composite structures with diffuse field conditions is presented. This technique based on time reversal approach, is directly applied to the experimental impulse responses of the structure recorded by only one passive sensor and stored into a database The proposed method allows achieving the optimal focalization of the acoustic emission source in the time and spatial domain as it overcomes the drawbacks of other ultrasonic techniques. Indeed, exploiting the benefits of a diffuse wave field, a high refocusing quality (spatial resolution), with only one sensor can be accomplished. The efficiency of this method is experimentally demonstrated on a stiffened composite panel. The results showed that the impact source location could be retrieved with a high level of accuracy in any position of the structure (maximum error was less than 3%).

References

[1] Ciampa F, Meo M. "Acoustic emission source localization and velocity determination of the fundamental mode A_0 using wavelet analysis and Newton-based optimization technique". *Smart Mater. Struct.* ***19***, 1-14 (2010).

[2] Tobias A. "Acoustic emission source location in two dimensions by an array of three sensors", *Non-Destructive Testing*, **9**, pp. 9-12 (1976)

[3] Meo M, Zumpano G, Pigott M, Marengo G. “Impact identification on a sandwich plate from wave propagation responses”. *Compos. Struct.* ***71***, 302-306 (2005).

[4] Ciampa F., Meo M. "A new algorithm for acoustic emission localisation and flexural group velocity determination in anisotropic structures". *Composites: Part A* (2010).

[5] Paget C A, Atherton K, O’Brien E. “Triangulation algorithm for damage location in aeronautical composite structures”. *Proc. of the 4th Int. Workshop on Structural Health Monitoring, Stanford, CA, 363-370* (2003).

[6] Weaver R. “On diffuse waves in solid media”. *J. Acoust. Soc. Am*. ***71*** *(6)*, 1608–09 (1982).

[7] Lobkis O.-I, Weaver R. “On the emergence of the Green's function in the correlations of a diffuse field”. *J. Acoust. Soc. Am*. ***110*** *(6)*, 3011–17 (2001).

[8] Dorme C, Fink M. “Focusing in transmit-receive mode through inhomogeneous media: The time reversal matched filter approach”. *J. Acoust. Soc. Am*. ***98*** *(2)*, 1155–1162 (1995).

[9] Derode A, Larose E, Tanter M, de Rosny J, Tourin A, Campillo M, Fink M. “Recovering the Green’s function from field-filed correlations in an open scattering medium (L)”. *J. Acoust. Soc. Am*. ***113*** *(6)*, 2973–2976 (2003).

[10] Fink M. “Time-reversal waves and super resolution”. *Journal of Physics: Conference Series*, vol. 124, p. 012004 (2008).

[11] Ing R.-K, Quieffin N, Catheline S, Fink M. “In solid localization of finger impacts using acoustic time-reversal process”. *Appl. Phys. Lett.* ***87***, 204104 (2005).

[12] Zumpano G, Meo M. “A new nonlinear elastic time reversal acoustic method for the identification and localisation of stress corrosion cracking in welded plate-like structures – A simulation study” *Int. J. Solids Struct.* ***44***, 3666–84 (2007).

[13] Barbieri E, Meo M. "Discriminating linear from nonlinear elastic damage using a nonlinear time reversal DORT method", *Int. J. Solids Struct.* (2010).

[14] Wang C.–H, Rose J.–T, Chang F.–K. “A synthetic time-reversal imaging method for structural health monitoring”. *Smart Mater. Struct.* ***13***, 415-423 (2004).

[15] Tanter M, Thomas J.-L, Fink M. “Focusing and steering through absorbing and aberrating layers: Applications to ultrasonic propagation through the skull”. *J. Acoust. Soc. Am*. ***103*** *(5)*, 2403–2410 (1998).

[16] Ribay G, Catheline S, Clorennec D, Ing R K, Queffin N, Fink M. “Acosutic Impact Localization in Plates: Properties and Stability to Temperature Variation”. *IEEE Trans. Ultrason. Ferroelectr. Freq. Control* ***54*** *(2), 378-85* (2007).